Research Article

Saman Sargazi*, Seyedeh Maryam Hosseinikhah, Farshid Zargari, Narendra Pal Singh Chauhana, Mohadeseh Hassanisaadi, and Soheil Amani

pH-responsive cisplatin-loaded niosomes: synthesis, characterization, cytotoxicity study and interaction analyses by simulation methodology

https://doi.org/10.1515/nanofab-2020-0100
Received Oct 16, 2021; accepted Oct 28, 2021

Abstract: Cisplatin (Cis) is an effective cytotoxic agent, but its administration has been challenged by kidney problems, reduced immunity system, chronic neurotoxicity, and hemorrhage. To address these issues, pH-responsive non-ionic surfactant vesicles (niosomes) by Span 60 and Tween 60 derivatized by cholesteryl hemisuccinate (CHEMS), a pH-responsive agent, and Ergosterol (helper lipid), were developed for the first time to deliver Cis. The drug was encapsulated in the niosomes with a high encapsulation efficiency of 89%. This system provided a responsive release of Cis in pH 5.4 and 7.4, thereby improving its targeted anticancer drug delivery. The noisome bilayer model was studied by molecular dynamic simulation containing Tween 60, Span 60, Ergosterol, and Cis molecules to understand the interactions between the loaded drug and noisome constituents. We found that the platinum and chlorine atoms in Cis are critical factors in distributing the drug between water and bilayer surface. Finally, the lethal effect of niosomal Cis was investigated on the MCF7 breast cancer cell line using 3-(4, 5-Dimethylthiazol-2-yl)-2, 5-diphenyltetrazolium bromide (MTT) assay. Results from morphology monitoring and cytotoxic assessments suggested a better cell-killing effect for niosomal Cis than standard Cis. Together, the synthesis of stimuli-responsive niosomes could represent a promising delivery strategy for anticancer drugs.

Keywords: Cis; Cytotoxicity; pH-responsive release; simulation; Niosome

1 Introduction

Although cancer has been discovered for a long time, it is still considered a multifaceted universal health matter and one of the indispensable challenges in medicine [1]. Among the different types of cancers, breast cancer is the most common cancer type in women [2]. Remarkable advance has been carried out to improve breast cancer treatment in the recent decades. However, the current clinical approaches such as chemotherapy, radiation therapy, and surgery show some disadvantages; these methods are invasive, have low specificity, and cause drastic side effects [3–10].

Several drugs have been recently studied as a single drug agent or in combination with other anti-cancer agents for targeted cancer therapy [11–14]. Among them, cisplatin (Cis) or cis-di-amminedicholoroplatinum (II) is considered a standard chemotherapy drug for the treatment of various human carcinoma including breast, refractory non-Hodgkin's lymphomas, liver, bladder, lung cancers [15, 16]. Its function mode has been related to its ability to link with purine bases of DNA, leading to DNA damage induction and, therefore, triggering apoptosis in tumor cells [15]. Due to several severe side effects of platinum drugs, such as kidney problems, reduced immunity system, chronic neurotoxicity, and hemorrhage, introducing novel strategies can benefit cancer patients [15]. Toward overcoming these side effects, several nanoparticles (NP) as drug carriers have been employed as drug delivery systems (DDSs) for Cis to

*Corresponding Author: Saman Sargazi: Cellular and Molecular Research Center, Research Institute of Cellular and Molecular Sciences in Infectious Diseases, Zahedan University of Medical Sciences, Zahedan 9816743463, Iran; Email: sgz.biomed@gmail.com
Seyedeh Maryam Hosseinikhah: Nanotechnology Research Center, Pharmaceutical Technology Institute, Mashhad University of Medical Sciences, Mashhad, Iran
Farshid Zargari: Pharmacology Research Center, Zahedan University of Medical Sciences, Zahedan 9816743463, Iran; Department of Chemistry, Faculty of Science, University of Sistan and Baluchestan, Zahedan 98135674, Iran
Narendra Pal Singh Chauhana: Department of Chemistry, Faculty of Science, Bhupal Nobles' university, Udaipur, 313002, Rajasthan, India
Mohadeseh Hassanisaadi: Department of Plant Protection, Shahid Bahonar University of Kerman, Postal Code: 7618411764, Kerman, Iran
Soheil Amani: Department of chemistry, Institute for Advanced Studies in Basic Sciences (IASBS), Zanjan, Iran

improve accumulation in tumor cells and reduce side effects [17–26]. A broad range of delivery systems have been utilized to deliver Cis into the target tissues, but there are few more effective tools for therapeutic purposes due to the drug's minor hydrophilic and hydrophobic properties [27–32]. Many polyethylene glycol (PEG)-coated liposomal nanoformulations, including Aroplatin, Lipoplatin, and SPI-077, are under clinical trial phases, with the encapsulating of Cis have been overcome the weak aqueous solubility, drug resistance, and toxicities [33]. Therefore, nanotechnology may bring pleasant opportunities to cancer treatment and diagnosis [34–43].

Niosomes are an effective nanocarrier utilized in drug delivery systems due to biodegradable, biocompatible, and non-immunogenic characteristics. They are classified as non-ionic surfactant vesicles and have the potential to target therapeutic agents directly to the tumor, improve the efficacy, and diminish the side effect of chemotherapy by selectively transporting drugs to tumor space [44]. Niosomes are considered stable bilayer vesicles created by the self-association process of non-ionic surfactants and lipid such as cholesterol in an aqueous medium [45]. Hydrophilic and lipophilic therapeutic agents are loaded into the aqueous core and membrane bilayer of noisome, respectively [45]. Niosomes can be classified into several groups based on their bilayers and sizes: 1) small unilamellar vesicles (SUV) with 10-100 nm, large unilamellar vesicles (LUV) with 100-3000 nm, and multilamellar vesicles (MLV) with having several bilayers [4, 45–54].

It is better to note that, among the nanocarrier systems sensitive to stimuli, pH is considered the most usually applied delivery stimuli. It has been utilized to release the drug parts under reformed pathological conditions, like several inflammations like cancer or ischemia with marked pH changes. The extracellular pH is generally conserved at around 7.4 in normal tissue and blood. Typical extracellular pH values usually are acidic because of the more glycolysis rates in several tumors. Low pH of tumor space can help drugs to be released into the target sites. pH-responsive nanocarriers, which can accept or donate H^+ at pathological pH, allow moderate structural changes to happen and are more commonly utilized for these systems [55]. Cosco and coworkers were encapsulated 5-FU in bola-niosomes, which were coated with PEG or were un-coated. They investigated this formulation on MCF-7 and T47D breast cancer cell lines. Both the formulations indicated more cytotoxic effects toward the free drug. *In vivo* results on MCF-7 xenograft tumor on the severe combined immunodeficient (SCID) mouse models indicated more effective antitumor activity of niosomal drug at a concentration 10 times less (8 mg/kg) than that of the free solution of the 5-FU (80 mg/kg) after a treatment of 1 month [56]. In another study, Gude *et al.* loaded Cis into niosome by employing cholesterol and Span 60, and then they studied the antimetastatic activity in the metastatic model of B16F10 melanoma. They reported that niosomal Cis has the remarkable antimetastatic effect and decrease adverse effect and toxicity compared to free Cis [57]. In a study, Yang *et al.* prepared niosomal Cis formulation and modified the system with cholesterol and Span 40. They reported that the diameter and the encapsulation efficiency were 7.73 ± 1.49 μm with a *zeta*-potential of 0 mV and 76.93 ± 2.67%, respectively. The antitumor efficiency was investigated in rabbits bearing VX2 sarcoma. The injection of niosomal Cis to rabbits inhibited tumor growth and resulted in much lower mortality than the free drug. The promising anticancer outcomes demonstrated that the niosomal Cis might be progressed as a suitable anticancer form of the drug with low toxicity [58]. Also, there is some related study about the encapsulation of Cis in liposome nanocarriers. For example, Cis-loaded liposome was combined with 6-amino nicotinamide to overcome drug resistance in ovarian cancer cells was developed. The combination treatment of liposomal Cis and 6-amino nicotinamide showed promising cytotoxic activities in drug-resistant cells and prolonged pharmacokinetics in rats [59]. Another study evaluated two novel liposomal formulations of Cis as potential therapeutic agents for treating glioma in the F98 rat glioma model. a variety of dose-dependent neuropathologic changes from none to severe were seen at 10 or 14 d following their administration. These findings suggest that further refinements in the design and formulation of Cis-containing liposomes will be required before they can be administered i.c. by convection-enhanced delivery (CED) for the treatment of brain tumors and that a formulation that may be safe when given systemically may be highly neurotoxic when administered directly into the brain [60].

Knowing drug delivery systems, especially the mechanism of drug encapsulation and release at the atomistic level, is required for designing new nanomedicines [48, 61–66]. A new field has emerged as computational pharmaceutics in which degradation, stability, preservation from the body's defensive mechanisms, drug release, and targeted distribution are all difficulties that computational techniques can help with [67]. In this manner, techniques such as Molecular Dynamics (MD) simulation technique and Monte Carlo simulations are powerful tools to understand how the atomistic interactions and forces can govern and develop new drug delivery systems [68].

In this study, Span 60, Tween 60, Ergosterol, and CHEMS were mixed to obtain pH-responsive niosome formulations loaded with Cis. Morphology, size, zeta potential, stability, entrapment efficiency (EE), and release behavior

were evaluated by different methods. Moreover, for simulation assessment, the noisome bilayer was initially constructed by Span 60, Tween 60, and Ergosterol using the CELL microcosmos 2.2 software by fetching the structures from PUBCHEM and then optimizing geometrically in HF/6-3G (d,p) level of theory. In the end, experiments were carried out to investigate the effect of Cis on the growth and metastasis of breast cancer as a free drug or an alkylating agent loaded in pH-sensitive niosomes.

2 Materials and Methods

2.1 Chemicals and cell line

Cis drug and MTT reagent were procured from Sigma-Aldrich (St Louis, MO, USA and St. Louis, MI, USA, respectively). Cholesteryl hemisuccinate (CHEMS) was obtained from Avanti Polar Lipids, Inc (Alabaster, Alabama, USA). Ergosterol, Span 60 and Tween 60 was procured from Sigma-Aldrich (Steinheim am Albuch, Germany and St Louis, MO, USA). Fetal bovine serum (FBS) and RPMI1640 culture medium were obtained from Gibco (Grand Island, NY, USA). Trypan blue, 1% penicillin/streptomycin, dimethyl sulfoxide (DMSO), trypsin-EDTA solution, and phosphate-buffered saline (PBS) were purchased from IN-OCLON (Tehran, Iran). The MCF7 human breast cancer cell line was provided by the Pasteur Institute of Iran (Tehran, Iran) and maintained in a culture medium containing 10% FBS, 1% penicillin/streptomycin mix, at 37°C with 95% humidity and 5% CO_2.

2.2 Preparation of pH-responsive Cis loaded niosomes

Niosomes containing Cis were prepared by a thin-film hydration technique. Briefly, Span 60, Tween 60, Ergosterol and CHEMS were dissolved in chloroform with an appropriate molar ratio. The solvent was evaporated using a rotary evaporator (Laboroa 4003, Heidolph, Germany) at 120 rpm and 60°C. The thin film formed at the bottom of the round bottom flask was then hydrated by ultrapure water containing 86 ppm of Cis and stirred until a milky solution was obtained. Niosomal formulations were centrifuged for 20 min at 15000 rpm (5415D, Eppendorf, Germany), and to provide smaller and more homogenized particles, they were sonicated using bath sonication (Thermo Fisher Scientific, USA) for 5 min. After that, the formulation was filtered 4 times with 0.45 and 0.22 um polycarbonate membrane filters (Sartorius AG, Göttingen, Germany). Blank niosomes were prepared with the method mentioned above, without the Cis. All the samples were stored at 4°C, protected

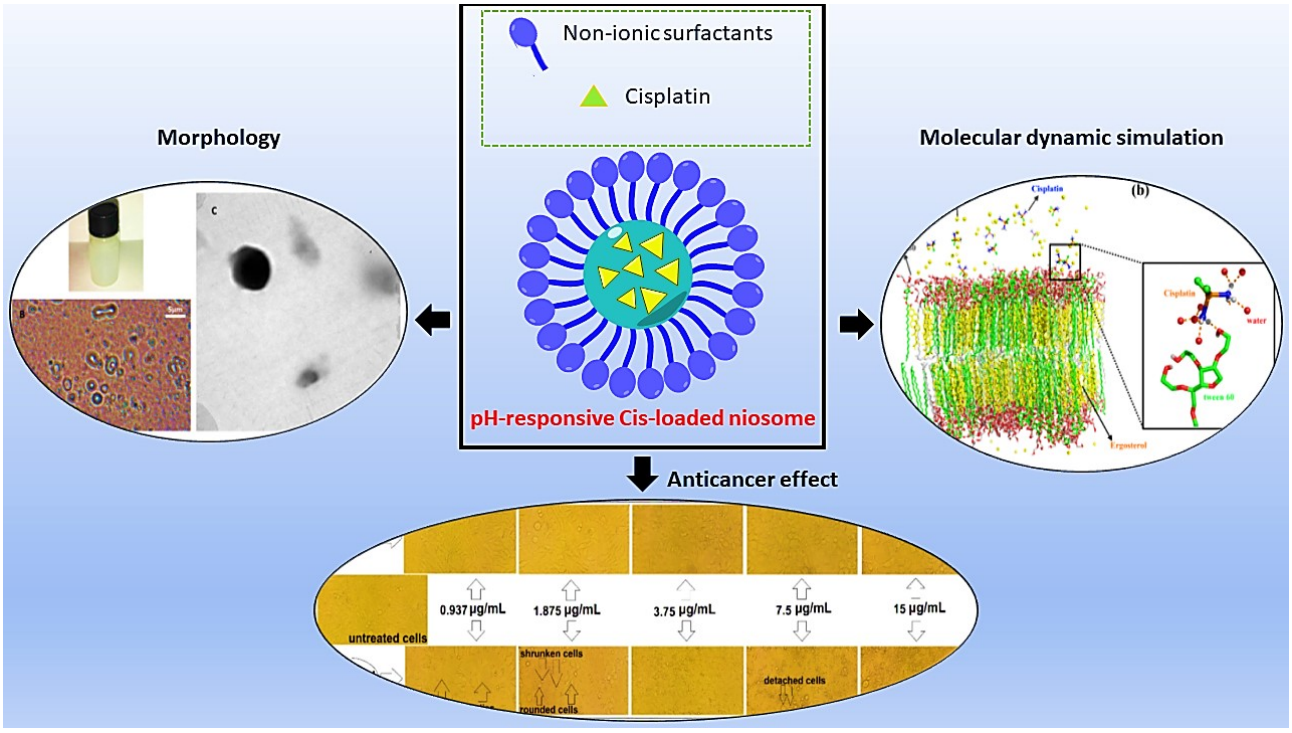

Scheme 1: Schematic representation of pH-responsive Cis-loaded niosomes.

from the light. A schematic representation of pH-responsive Cis-loaded niosomes was given in Scheme 1.

2.3 Simulation study

2.3.1 Forcefield setup and parametrization

Due to the permanent role of Cis in the initiation of apoptotic routes, resistance mechanisms, and delivery of the drug, it is crucial to characterize these interactions with lipid membranes. The prerequisite is a simplified model to facilitate the evaluation of these interactions and to be accurate enough at the same time.

The parameters for each component of the noisome bilayer were described by the Lipid 17 force field, which is a developed version of lipid 14 forcefield for lipids [69]. The structures of span 60, tween 60, and Ergosterol were optimized in HF/6-3G (d,p) level of theory to obtain the geometrically most reliable structure and extract each atom's atomic partial charge using Restrained Electrostatic Potential (RESP) charge methodology [70]. Conversion of Assisted Model Building with Energy Refinement (AMBER) topology and coordinate file into the GROMACS has been done with the ACPYPE python tool [71].

Force field parameters for Cis, including bond, angle and dihedral were obtained using the *MCPB.py* module [72] of AmberTools20 [73]. To extract the atomic charge based on the RESP charge method, the output of geometrically optimized structure of Cis at the B3LYP/aug-cc-pV5Z-PP (using effective core potential) level for platinum atom and 6– 311++G** level of theory for other atoms was employed.

2.3.2 Bilayer setup and simulation details

The noisome bilayer was initially constructed by span 60, tween 60, and Ergosterol using the CELL microcosmos 2.2 software [74] by fetching the structures from PUBCHEM and then optimizing geometrically in HF/6-3G (d,p) level of theory. The structures of different niosome components are represented in Figure 1. The number of each molecule with the 35:35:30 molar ratio for the building of the bilayer were 159,161 and 138 molecules for tween 60, span 60, and Ergosterol, respectively. All bilayer components were placed randomly in a box area of 7.80 nm × 7.80 nm, with the hy-

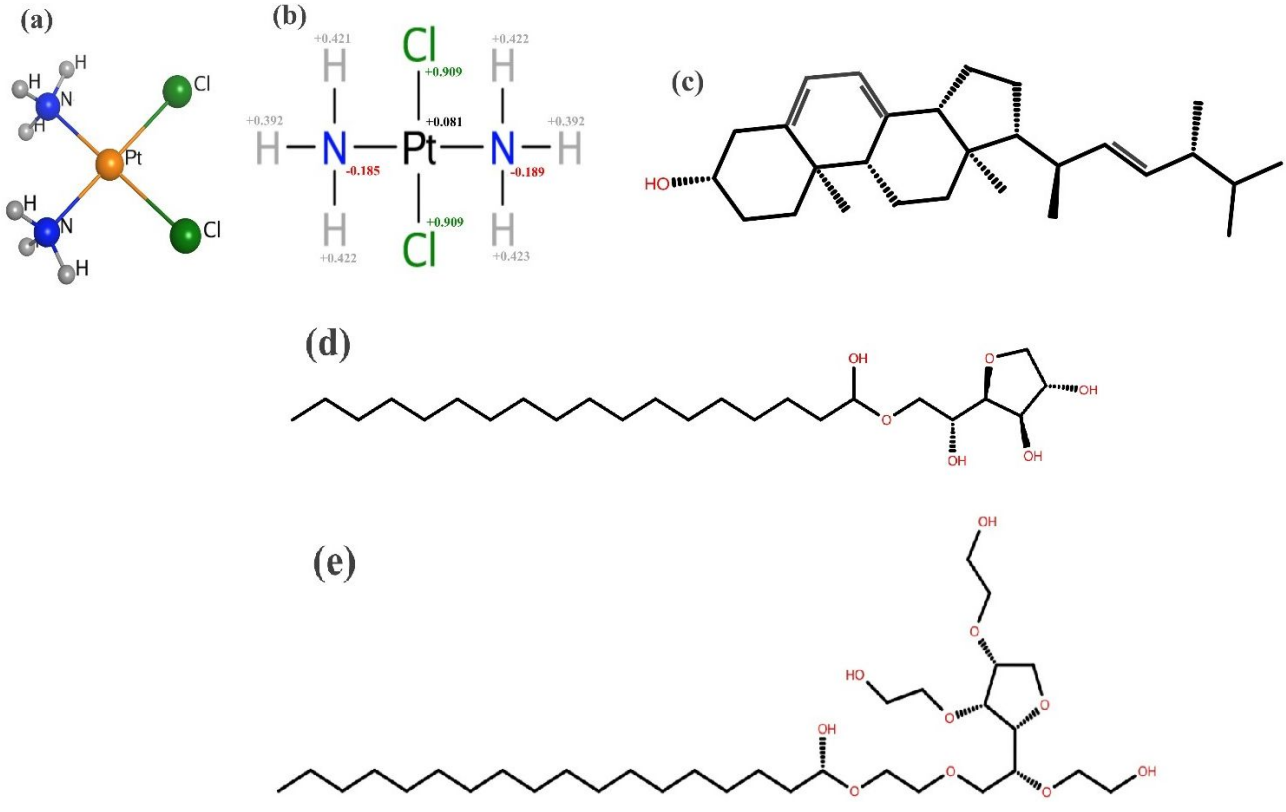

Figure 1: The (a) 3D and (b) 2D structure of Cis with atomic charge calculated for each atom.2D structure of (c) Ergosterol (d) span 60 and (e) tween 60 with the numbering of atoms based on the amber nomenclature.

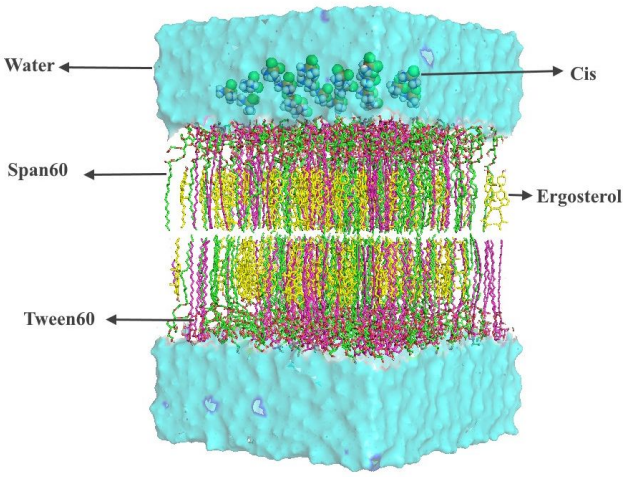

Figure 2: The starting structure of the noisome bilayer contains 20 Cis drugs at the top. Span60, tween60, and Ergosterol molecules are colored green, purple, and yellow, respectively. The Cis molecules are represented as the Space-filling model.

drophilic heads and hydrophobic parts placed inversely towards each other in the box.

As shown in Figure 2, 20 numbers Cis molecules were inserted in the upper leaflet of the bilayer to investigate the interactions of these molecules with the noisome bilayer. The final structure was solvated in an SPC/E water box as this model can accurately reproduce the water's surface tension [75]. The whole system was subjected to energy minimization using the steepest descent algorithm to avoid the unexpected overlap between atoms in the constructed noisome bilayer. A short simulation annealing was conducted in 500 K for 100 ps to remove the remaining clashes among atoms in the box. The system was subsequently subjected to NVT simulation run for 500 ps at 298 K to equilibrate the system's temperature. The choice of this temperature corresponds to optimal conditions for the formation of niosome vesicles that show the highest stability [76]. In this step, the Span 60, tween 60 and Ergosterol, were coupled together to the v-rescale thermostat with a coupling constant of 0.1 ps while the water and Cis were coupled separately. The resulting configuration was then subjected to 5 ns of NPT simulation using Berendsen barostat with semi-isotropic coupling to keep the temperature and the system's pressure constant at 298 and 1 bar, respectively. The periodic boundary conditions were applied in all three directions. Bond constraints were applied using the Linear Constraint Solver (LINCS) algorithm [77], and The electrostatic interactions were calculated using the fast Particle Mesh Ewald method (PME) method [78]. Cut off for the Coulomb, and van der Waal interactions were assigned to 1.5 nm. The systems were simulated for 100 ns production run in Gromacs 2020.1 package.

2.4 Size and zeta potential Measurement of niosomes

The size and zeta potential of niosomes were calculated using Zetasizer (Malvern, Helix, UK). Briefly, niosome formulation was diluted 10 times and assessed by dynamic light scattering (DLS) instrument at the autocorrelation function of 90°, laser operating at 658 nm, a light source of 35 mW, and temperature of 25°C.

2.5 Morphological evaluation of nanoparticles

Optical microscopy (before size reduction) and transmission electron microscope (TEM)(After size reduction) was used to analyze the morphology of niosome formulations. For TEM, A drop of the formulation was placed onto a carbon-coated copper grid, then air-dried, and examined under a transition electron microscope (EM10C, Zeiss, Germany).

2.6 Encapsulation efficiency

To this purpose, a niosome containing Cis was centrifuged (15000 rpm, 1 hour and 4°C), and the supernatant was obtained. The concentration of Cis in the supernatant was calculated using a standard curve at 310 nm by spectrophotometer, and then the drug loading and encapsulation efficiency were estimated based on total concertation of Cis and concentration of Cis in the supernatant.

2.7 Drug release from niosome in different pHs

To estimate the drug retention capability of the niosome, sediment of Cis-loaded niosome formulation was obtained using centrifugation process (15000 rpm, 1 hour, and 4°C). The sediment of the formulation containing Cis was resuspended into fresh ultrapure water and poured into a dialysis bag (Cut off; 12,000 Da Sigma), immersed into 50 ml PBS (pH 5.4 and 7.4), and stirred (100 rpm, 37°C). At the predetermined time intervals, 1 ml of buffer solution was withdrawn and replaced with a fresh one. The release rate of the drug was estimated, and the relative curve was plotted.

2.8 Cytotoxicity and morphology assessments

Free Cis and niosomal Cis were applied into the culture medium at increasing concentrations. MCF7 cells were exposed to of 0.469, 0.937, 1.875, 3.750, 7.5, 15 and 30 µg/mL of both drugs. Cytotoxic effects of free and encapsulated Cis were examined using the 3-(4, 5-Dimethylthiazol-2-yl)-2, 5-diphenyltetrazolium bromide (MTT colorimetric assay as described before [79]. Briefly, 5×10^3 cells were seeded in every well of a 96-well microplate in a final volume of 100 µL. After 24 h, 100 µL of free and/or niosomal Cis (prepared as described above) was added to each well and allowed to grow in the following 24, 48, and 72 hours. Then, the culture medium was removed, and 200 µL of MTT solution (0.5 mg/mL in PBS) was added. After 4 h incubation at 37°C, the supernatant was replaced with 200 µL of DMSO. The absorbance of sample wells (treated) and control wells (untreated) was read at 570 nm using a SpectraMax microplate reader (Molecular Devices, Sunnyvale, CA) to determine the number of viable cells that reduced the tetrazolium component of MTT to formazan crystals. The experiment was repeated three independent times. The 50% inhibitory drug concentrations (IC50s) were assessed by GraphPad Prism version 7.0 for Windows (GraphPad Software, La Jolla, CA, USA).

Cell morphology was monitored using an inverted microscope (Model IX71, Olympus, Tokyo, Japan) at 40X magnification. For this purpose, cells (2×10^4 cell/well) were cultivated in a 24-well cell culture plate and incubated overnight. Next, cells were treated with escalating concentrations of free and niosomal Cis from 0.937 to 15 µg/mL for 48 h. Images were captured using a digital camera.

2.9 Statistics

The data were presented as a mean ± standard deviation. In each group, each value is the average of at least three separate tests. The student's t-test was used for statistical data. To demonstrate a significant difference, a $p<0.05$ significance value was chosen.

3 Results

3.1 Characterization of pH-responsive Cis-loaded niosomes

The niosome loaded with Cis was successfully prepared by the TFH method. Determinations were made of the particle size, size distribution (PDI), and surface charge. The average niosome size was around 90± 2 nm, and the uniform dispersion of particles (PDI: 0.28 ± 0.02) indicated a homogenous size distribution (Figure 3A). Through the increased permeability and retention (EPR) mechanism, the size of the niosomes is optimal for tumor-specific accumulation. Furthermore, after 4 months of storage at 4°C, there was a size increase of less than 15 nm, indicating that Cis-niosomes remained stable (data not shown). The negative

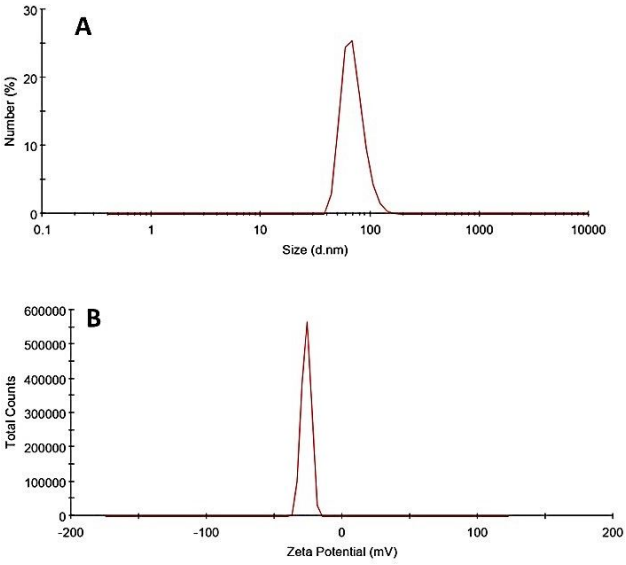

Figure 3: Size, Size distribution (A), and Zeta Potential (B) evaluation of pH-responsive Cis-loaded niosome by DLS at 25°C.

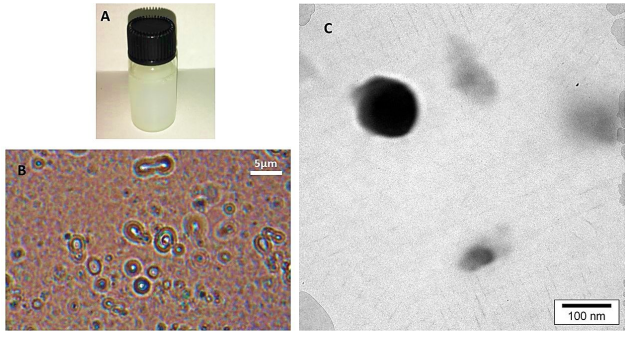

Figure 4: Physical appearance (A), Optical micrographs (100X magnification), and TEM image (C) of pH-responsive Cis-Loaded niosome.

surface charge of −31.2 mV evidenced the stability of the system (Figure 3B).

A sonication and filtration procedure was carried out to manufacture small niosomes with homogeneous size and dispersity and to reduce aggregation. The hydrated medium containing niosomal Cis is shown in Figure 4A. It has a milky white appearance without any aggregation. Optical microscopy characterized the synthesized niosomes in various spherical shapes, and the formed niosomes were typically circular MLVs morphologically, as seen in Figure 4B. This was expected, as MLVs are typically produced via the film hydration approach. The pH-responsive Cis-loaded niosomes displayed homogenous spherical forms and smooth surfaces without any aggregated particles, as shown by TEM images (Figure 4C). The diameters of the niosomes lowered as the sonication and filtration process were used.

The difference between the free Cis (nonencapsulated) and total Cis was used to calculate the encapsulation efficiency percentage of the developed formulation. The absorbance reads were converted to concentration using a calibration curve, prepared for Cis. Our prepared niosome formulation had an encapsulation efficiency of 89% that is remarkably high; thus, we recommend encapsulating Cis with the thin-film hydration method.

3.2 In-vitro Cis release in pH 5.4 and 7.4

In drug release behavior, the type of entrapped agent, vesicle lamellarity, and existence or absence of the pH-responsive agent must all be taken into account in niosomal formulations and other drug delivery systems. Drug transport from vesicles is also influenced by the chemical composition of the noisome bilayer. The biphasic drug release profile of niosomal systems indicates fast desorption and slower diffusion of the entrapped drug via bilayer phases. A similar biphasic release was observed in the present study for pH-responsive niosome at pH 5.4 (Figures 5). The rapid initial phase may be related to the effect of CHEMS as a pH-responsive agent (about 83% release after 24 hours). For pH 7.4, a slower Cis release was observed during 24 hours which was due to diffusion of Cis from the lipid bilayer (about 46% after 24 hours). Based on results, Cis-loaded formulation showed a sustained release comparison to free Cis that released about 95% after 5 hours.

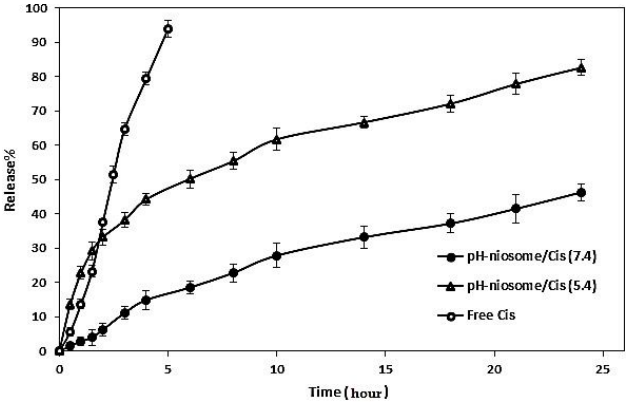

Figure 5: The profile of Cis release from pH-responsive Cis-Loaded niosome in pH 5.4 and 7.4 compared to the standard drug in phosphate buffer at 37°C (mean ±SD, n=3).

3.3 Simulation study

3.3.1 Bilayer structure

One of the main properties related to membrane bilayer is area per lipid (APL), by which one can evaluate the phase transition of the lipid bilayer as well validation of the force-field. However, we calculated the APL using the xy-surface area of the simulation box divided by the number of span 60, tween 60, and Ergosterol in on leaflet. Table 1 compares the structural properties, APL, and bilayer thickness of the noisome bilayer component used in this work at the beginning and the end of simulation time. The span60 has an average APL of 26.69 ± 0.1 $Å^2$ at the beginning of MD simulation, while this value diminished to 24.26± 0.1 $Å^2$ at the end which has a fair consistency with the experimental value (22 $Å^2$) [80]. Insertion of tween60 and Ergosterol to the span60 bilayer, which is closely packed with high order orientation, do not expand the bilayer at all. Tween 60 and Ergosterol possessed an average APL of 24.82± 0.1 and 28.08 ± 0.1 $Å^2$ after 40 ns MD simulation.

The bilayer thickness is another structural property of the bilayer system, which is defined as the center of mass of the headgroup of every bilayer component, *i.e.*, span60, tween60, and Ergosterol. The calculated thicknesses at the beginning and the end of the simulation for each component are represented in Table 1. It is seen that the bilayer thickness for span60, tween60 and Ergosterol, were 7.92 ± 0.001, 8.95 ± 0.001, and 4.85 ± 0.001 at the end of the simulation. The GridMAT-MD script [81] was utilized to calculate APL and thickness of each lipid in the noisome bilayer.

Table 1: Comparison of the structural properties of Span60, Tween60, and Ergosterol bilayers in 35:35:30 %mol at the beginning and the end of the MD simulation.

lipid	Span60		Tween60		ergosterol	
time	0 ns	100 ns	0 ns	100 ns	0 ns	100 ns
Area per lipid ($Å^2$)	26.69 ± 0.1	24.26± 0.1	28.31± 0.1	24.82± 0.1	30.92 ± 0.1	28.08 ± 0.1
Thickness (nm)	7.78 ± 0.001	7.92 ± 0.001	8.03 ± 0.001	8.95 ± 0.001	4.75 ± 0.001	4.85 ± 0.001

3.3.2 Hydrogen bonding between membrane and Cis

To identify the number and/or duration of hydrogen bonds formed between three components of noisome bilayer-span60, tween60, and Ergosterol with Cis, we utilized the hydrogen bond analysis during the 100 ns of trajectory period. Hydrogen bond profiles between the Cis and the lipids were calculated using the H-bond utility of Gromacs 2020.2. The threshold for H-bond forming was 3.5 Å with an angle of 30. Figure 6a illustrates the average position of the Cis on one side of the bilayer during the 100 ns MD simulation. According to this figure and other snapshots from MD simulation, we realized that Cis intends to interact with water molecules and resides in MLV space in niosome. Our visual inspection from MD simulation snapshots revealed the interaction of Cis with the Tween 60 headgroup. Figure 6b represents such an interaction in detail. In this figure, the ammoniumyl groups in Cis make H-bonds with O8 atom of tween 60 headgroup. Due to the high electrophilicity of hydrogens in ammoniumyl groups in Cis, we would expect this interaction as well as hydration of Cis with water molecules during the simulation.

More detailed analyses of hydrogen bonds between Cis and Span60, Tween60, and Ergosterol have been shown in Table 2.

Based on the data reported in Table 2, the average H-bonds between Cis and span 60 and tween 60 is 0.004 and 0.045 during MD simulation. This is in line with our visual inspection of drug-bilayer interactions, which states that most of H-bond between Cis form through the tween 60 headgroup while the span 60 associated in minority and Ergosterol showed none contacts with Cis at all. The oc-

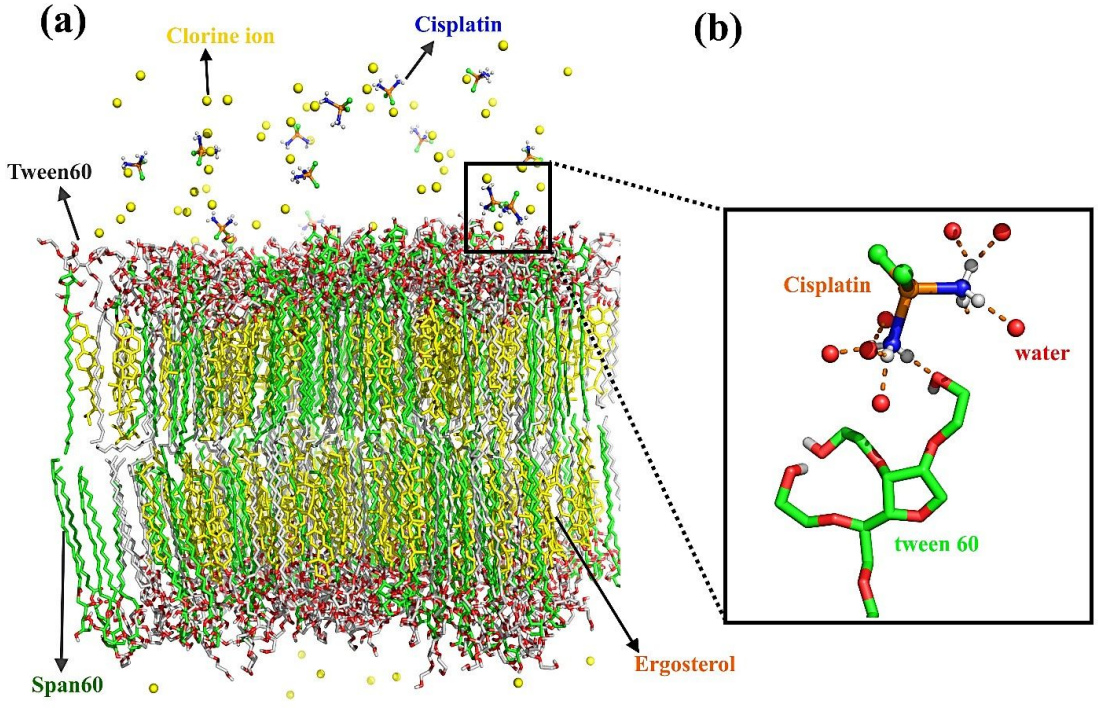

Figure 6: (a) Molecular representative structure of Cis in contact with niosome bilayer as facial representation and (b) the close-up representation of Cis at the surface of bilayer and the most probable hydrogen bonds between it and bilayer components. Carbon atoms in Span 60, tween 60 are colored green and grey, respectively. The Cis and chloride ions are represented as ball and stick. The platinum chlorine atoms in Cis and chloride ions in balk water are colored orange, green, and yellow, respectively.

Table 2: Average and detailed hydrogen bond analysis of Cis with span60, tween60, and Ergosterol in this study.

	Hydrogen Bonds					
	Cis-Span60		**Cis-Tween60**		**Cis-Ergosterol**	
Average H-Bond number	0.004		0.045		0.0	
	Donor-Acceptor	**Occupancy**	**Donor-Acceptor**	**Occupancy**	**Donor-Acceptor**	**Occupancy**
Detailed hydrogen bonds	Cis@N4-SPA@O1	0.28	TWE@O8-Cis@N4	1.83		
	SPA@N3-Cis@O1	0.10	TWE@O8-Cis@N3	1.87		
	SPA@N3-Cis@O4	0.02	TWE@O10-Cis@N4	0.50		
	Cis@N4-SPA@O4	0.01	TWE@O10-Cis@N3	0.19		

SPA: span60 TWE: tween60 ERG: Ergosterol Cis: Cisplatin

cupancy numbers are related to the lifetime of hydrogen bond between O1 and O4 atoms of span60 with nitrogen atoms of ammoniumyl group in Cis. The occupancy numbers for span 60 are smaller than those related to tween 60, and it also reveals that the O8 atom in tween 60 has maximum occupancy due to its higher exposure to Cis and water phase.

3.3.3 Radial distribution function analysis

The conventional definition of hydrogen bonds and ineligibility of many software to measure unconventional h-bonds leads us to investigate the interaction of other atoms in Cis with niosome bilayer components. The interactions involved other Cis atoms in the Cis-niosome system formations can give us additional structural insight and can be assessed by average radial distribution functions (RDF) plots of the Cis, span60, tween60, and the Ergosterol. Figure 7 shows such RDF plots for these systems. For evaluating the interaction of platinum and chlorine atoms in Cis, we performed RDF calculations towards headgroups atoms of span60 (O1, O4) and tween 60 (O8 and O7).

The hydrogen bond analysis persuades us to think that the ammoniumyl groups in Cis have predominant interaction between Cis and niosome components. As demonstrated in Figure 7a, and based on RDF calculation for all pair atoms, we can see that it is a platinum atom that strongly interacts with a span 60 headgroup including O1 and O4 atoms. These strong interactions are happening in distances lower than 1 Å. The lack of interaction with tween 60 headgroup states that Cis is strongly interacting with span 60 headgroup through its platinum and chlorine atoms. Figure 7b shows the RDF plots regarding atom O8 in tween 60 headgroup interacting strongly with chlorine atom in Cis, which makes speculation about interacting of tween 60 with chlorine atom in Cis.

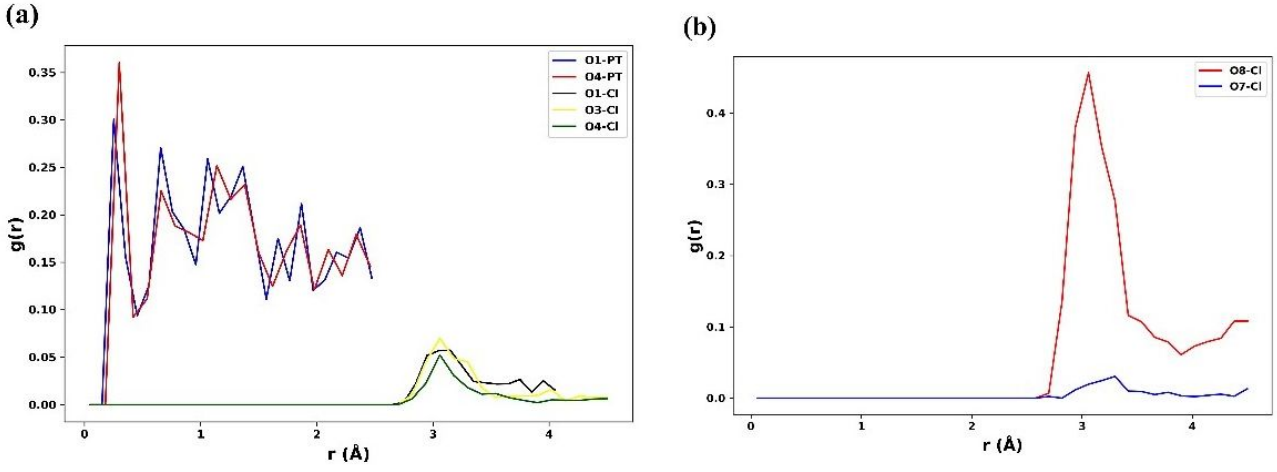

Figure 7: The atom-atom RDFs of (a) the span 60 and (b) tween 60 headgroup atoms with atoms in Cis molecules. The most probable interactions are represented here.

3.4 Lethal effects of niosomal cis

Figure 8 shows the results of the MTT assay of free and niosomal Cis. Compared to untreated cells, both agents significantly decreased the number of viable MCF7 cells ($P < 0.05$) following time- and dose-dependent fashions. We found that niosomal Cis was more cytotoxic than free Cis. In other words, IC50s were less in encapsulated Cis than in its free form. After 48 h treatment, the percentage of viable MCF7 cells treated with 0.469, 0.937, 1.875, 3.750, 7.5, 15 and 30 µg/mL of niosomal Cis was 65.7, 36.1, 29.7, 14.3, 6.4, 4.3, and 2.2%, respectively. Following 24, 48, and 72 h treatment, the IC50 values for exposing MCF7 cells to free Cis were 10.54, 6.80, and 4.38 µg/mL, while these values were 1.02, 0.70, and 0.38 µg/mL for cells exposed to niosomal Cis, respectively.

Microscopic evaluation of cell morphology revealed that untreated MCF7 cells had normal morphology and were attached to the culture flask. Treatment with 0.937 to 15 µg/mL of free Cis did not induce noticeable morphological change, except for a moderate decrease in the number of viable cells. In contrast, niosomal Cis-treated cells were undergone evident morphological changes after 48 h. In this regard, exposing MCF7 cells to 0.937 µg/mL of niosomal

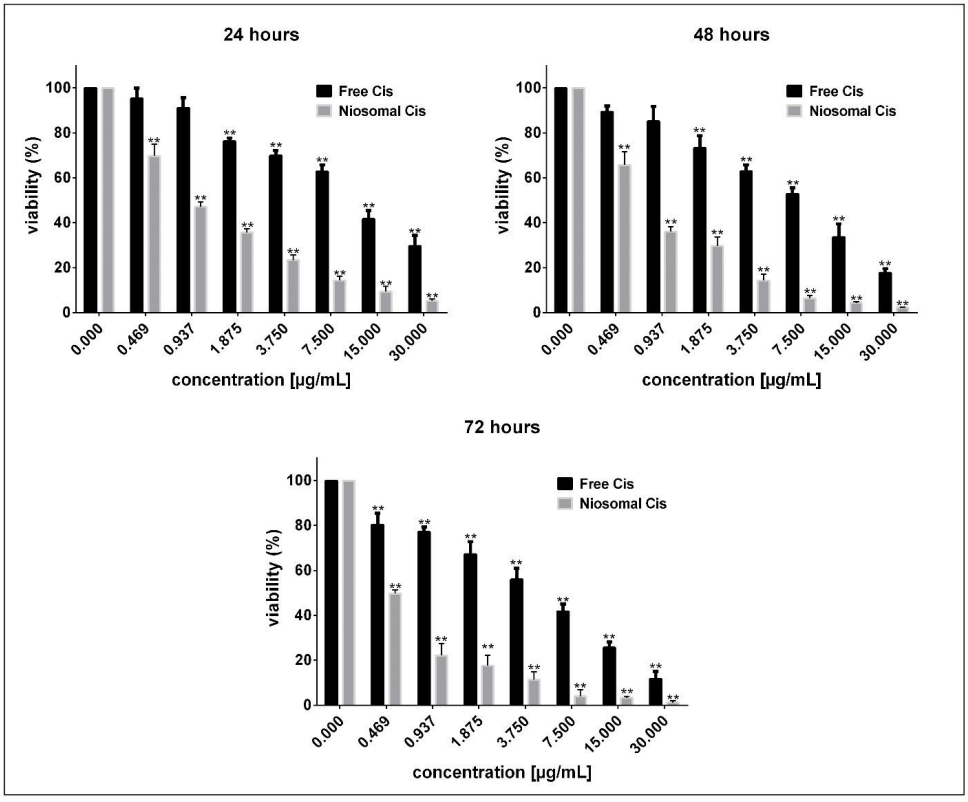

Figure 8: Lethal effects of free- and niosomal Cis on MCF7 breast cancer cells assessed via MTT test. Results were expressed as the average of three independent (mean±SD) (**P < 0.05* compared with untreated cells).

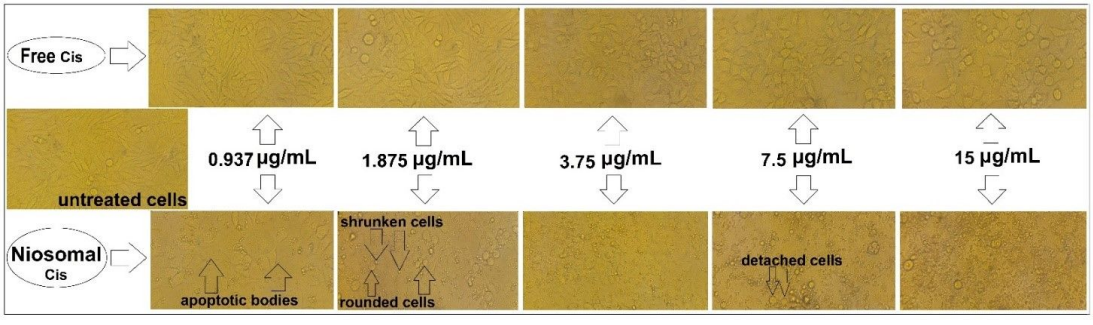

Figure 9: Morphology of MCF7 cells treated with 0.937-15 µg/mL of free and niosomal Cis for 48 h.

Cis induced the formation of apoptotic bodies. By increasing concentrations to 1.875 µg/mL, cells were rounded and shrunk. At higher concentrations of niosomal Cis (3.75 > µg/mL), cells were mainly detached from the culture dish, and many dead cells were floating in the culture media. This was not observed when cells were exposed to free Cis at given concentrations (Figure 9).

4 Discussion

Chemotherapy is a mainstay to treating various cancers. However, it has suffered many challenges, such as poor tumor selectivity and multidrug resistance (MDR). Targeted drug delivery via nanotechnology materials has afforded a new approach to solve the shortcomings. Niosomes are a promising drug delivery system since they can act as a reservoir for drugs and control drug release by changing their compositions [3, 28, 82–87]. There are various formulations of niosome containing chemotherapeutics in the literature. For example, Dabbagh Moghaddam *et al.* used melittin, as a peptide part of honey bee venom, which is considered a natural substance for cancer therapy. They loaded melittin into niosome and investigated the anticancer activity on 4T1 and SKBR3 breast cancer cell lines *in vitro* and *in vivo*. The formulation had been injected into BALB/C inbred mice. Several biological processes such as hemolysis, apoptosis, and cell cytotoxicity were investigated on 4T1 and SKBR3 cell lines by utilizing hemolytic activity assay, flow cytometry, MTT assay. The niosomal melittin can affect the expression of genes, down-regulates the expression of B-cell lymphoma (*BCL2*), Matrix metalloproteinases 2 (*MMP2*), and *MMP9* genes. They have also increased the apoptosis level and prevented cell migration, invasion in both 4T1 and SKBR3 cell lines compared to the melittin samples. Results of histopathology showed reduce mitosis index, invasion, and pleomorphism in melittin-loaded niosome. The study effectively states that niosomal melittin had more antitumor activities than melittin alone. This research has indicated that niosomes can be effective nanocarriers for melittin compared to the free form [88]. In another investigation, Mandriota *et al.* prepared a good nanostructure by using magnetic nanocrystal clusters (MNCs) as a superparamagnetic nanocluster. The size and density of nanoclusters and magnetic cores were investigated, respectively. After that, MNCs were modified with a polydopamine film (MNC@PDO) to increase their stability in an aqueous environment. Furthermore, they used polydopamine to enhance functional groups' density and get an appropriate nanosystem to drug-controlled release. As the final section of their research, Cis was attached to the surface of MNC@PDO to use the platform as a magnetic field-guided antitumor delivery system. The cytotoxic effects and the biocompatibility of MNC@PDO and MNC@PDO-Cis complexes were tested against both human cervical carcinoma (HeLa) and human breast adenocarcinoma (MCF-7) cells. *In vitro* investigations indicated that the MNC@PDO–Cis complexes prevented cellular growth by a dose-dependent effect. So, by using an external magnetic field, the drugs can release on a specific target zone. In summary, the nanosystem of MNC@PDO can be considered a valuable and potential nanocarrier for the delivery of several drugs to target sites [89]. Gude *et al.* designed niosomal formulations of Cis utilizing span 60 as excipient and cholesterol. Then, they studied the antimetastatic effect in an experimental metastatic model of B16F10 melanoma. They have also investigated theophylline and its combination outcome with free Cis and niosomal in the same model. As a result, treatment with niosomal Cis and combination of the same with theophylline exhibited a remarkable decrease in the nodules of the lung as compared to untreated control as well as with Cis alone. Furthermore, they treated with activated macrophages, which were activated using Muramyl dipeptide, significantly prevented more proliferation of tumours in the lung. Niosomal Cis indicated a major safety against weight loss and the effect of toxicity in bone marrow as compared to free Cis. These results can prove that Cis loaded in niosomes has a remarkable antimetastatic effect and diminished toxicities than Cis alone. However, theophylline did not show antimetastatic activity alone or combined with Cis or activated macrophages [57]. In another research, Doijad *et al.* intended to improve the efficacy, decrease toxicity and increase the therapeutic efficiency of niosomal Cis. At first, they were prepared niosomes by applying spans and tweens as excipients. Then, the formulations were characterized with a size distribution, entrapment efficiency, and *in-vitro* and *in-vivo* studies. The entrapment efficiency of the noisomes was obtained to be 66.66%, 54.16%, 60.80%, and 50.83% for span-60, span-80, tween-60, and tween-20, respectively. Furthermore, maximum cumulative percent drug release was reported with span-60 (96.87%) and the minor with tween-20 (70.49%) in 12 hours. The *in-vivo* result shown that the drug is especially targeting to liver followed by the spleen and lungs [90].

Nanometric size range, negative zeta potential, and high EE were obtained for niosome formulation. However, further studies are needed to produce better Cis-containing niosomes with maximum loading and efficiency to be used as a better candidate in the treatment of several cancers. To study the pattern of drug release, the dialysis tubing method was used. The release process of Cis-containing

niosome showed a sustained and pH-responsive release. According to the obtained results, it can be suggested that most of the drug release occurred at the first 4 hours at pH 5.4, but for pH 7.4, it was prolonged.

Based on *in vitro* cytotoxicity assay, we found that niosomal Cis exhibited better cytotoxic effects than free Cis (lower IC50s). Furthermore, encapsulated Cis induced marked morphological alterations in MCF7 cells that are hallmarks of apoptotic cell death. However, more *in vitro* studies are needed to determine the main mechanism of cell death activated by our newly prepared niosomal Cis. Cis has been shown to trigger apoptotic cell death via the endoplasmic reticulum-mediated pathway in breast cancer cells [91]. As biocompatible/biodegradable nanoparticle drug carriers, niosomes can transport drugs to desired tissues in the body [92]. Kanaani *et al.* examined the *in vitro* efficacy of nanoniosomated Cis on BT-20 human breast cancer cells and found nanoniosomated Cis exhibited a 1.5 fold greater cytotoxicity than standard Cis [93]. In 2012, Yang and colleagues loaded Cis into niosomes and modified the system with cholesterol and Span 40. Their findings indicated that niosomal Cis exerted much lower mortality and significant tumor growth inhibition in sarcoma-bearing rabbits [94].

On the other hand, the use of Cis is limited due to its side effects [95]. Gude *et al.* showed that niosomal Cis enhanced the lethal effects of theophylline in the murine B16F10 melanoma model [96]. MTT results of the present study were in agreement with these findings. Therefore, encapsulating Cis in niosomal formulation might be a desirable strategy to reduce the toxicity of standard Cis.

Based on our previous studies, the pH-sensitive niosome has a good *in-vivo* function. For better understanding of the efficacy of Cis-loaded niosomes, performing the *in-vivo* toxicity studies are encouraged. Despite numerous studies and concerning the fact that niosomes have a long way to go to pass the stage of clinical reality, there are still multiple challenges regarding the niosomes. For several reasons (stability, cost, etc.), niosomes are better than liposomes for drug delivery [97]. Surfactants as building components of niosomes have the most crucial role in the formation and properties of these carriers; thus, any developments in the synthesis of new surfactants that are nontoxic, low-cost, biocompatible, and biodegradable will increase the efficiency of niosomes. Therefore, it can be hoped that the special structures of the niosomes will arise in the coming years [98].

5 Conclusion

In the current study, a new pH-responsive Cis-loaded niosome formulation was developed to responsively and effectively deliver Cis for breast cancer treatment. It was demonstrated that niosomes provided a nanometric range, high stable formulation, and excellent entrapment efficiency of Cis. Moreover, the developed formulation showed a pH-responsive release at pH 5.4 and 7.4. The MD simulation results also showed that the interactions between Cis and noisome are mainly through its platinum and chlorine atoms with noisome components, especially tween 60 and span 60 headgroups. The prepared niosomes loaded with Cis exhibited better cytotoxic effects than standard Cis against breast cancer cells. Taken together, Cis-niosomes are potential delivery formulations for the treatment of breast cancer.

Funding information: This study received funding from Zahedan University of Medical Sciences (Project. 10267).

Authors' contributions: Conceptualization, S.S.; Methodology, S.S., S.M.H., F.Z., N.P.S.C., and M.H.; Investigation, S.S., S.A., and S.M.H, and F.Z.; Writing-original draft preparation, S.S., F.Z., F F.Z., N.P.S.C., and M.H.; Writing-review and editing, S.S.; Supervision, S.S.; Funding, S.S. All authors have read and agreed to the published version of the manuscript.

Conflict of interests: The authors declare no conflict of interest.

Ethical approval: The *in vitro* part of the study protocol was approved by Zahedan University of Medical Sciences (Ethical code: IR.ZAUMS.REC.1399.517).

References

[1] Kanaani L, Tabrizi MM, Khiyavi AA, Javadi IJAPJoCB. Improving the Efficacy of Cisplatin using Niosome Nanoparticles Against Human Breast Cancer Cell Line BT-20: An In Vitro Study. 2017;2(2):27-9.

[2] Tang X, Loc WS, Dong C, Matters GL, Butler PJ, Kester M, *et al.* The use of nanoparticulates to treat breast cancer. Nanomedicine. 2017;12(19):2367-88.

[3] Rahdar A, Hajinezhad MR, Hamishekar H, Ghamkhari A, Kyzas GZ. Copolymer/graphene oxide nanocomposites as potential anticancer agents. Polymer Bulletin. 2020:1-22.

[4] Alijani HQ, Iravani S, Pourseyedi S, Torkzadeh-Mahani M, Barani M, Khatami M. Biosynthesis of spinel nickel ferrite nanowhiskers and their biomedical applications. Scientific Reports. 2021;11(1):1-7.

[5] Amiri MS, Mohammadzadeh V, Yazdi MET, Barani M, Rahdar A, Kyzas GZ. Plant-Based Gums and Mucilages Applications in Pharmacology and Nanomedicine: A Review. Molecules. 2021;26(6):1770.
[6] Arkaban H, Ebrahimi AK, Yarahmadi A, Zarrintaj P, Barani M. Development of a multifunctional system based on CoFe2O4@ polyacrylic acid NPs conjugated to folic acid and loaded with doxorubicin for cancer theranostics. Nanotechnology. 2021;32(30):305101.
[7] Barani M, Bilal M, Rahdar A, Arshad R, Kumar A, Hamishekar H, et al. Nanodiagnosis and nanotreatment of colorectal cancer: An overview. J Nanoparticle Research. 2021;23(1):1-25.
[8] Barani M, Bilal M, Sabir F, Rahdar A, Kyzas GZ. Nanotechnology in ovarian cancer: Diagnosis and treatment. Life Sciences. 2020:118914.
[9] Barani M, Mirzaei M, Mahani MT, Nematollahi MH. Lawsone-loaded Niosome and its Antitumor Activity in MCF-7 Breast Cancer Cell Line: A Nano-herbal Treatment for Cancer. DARU J Pharm Sci. 2018;26:1-7.
[10] Barani M, Mirzaei M, Torkzadeh-Mahani M, Adeli-Sardou M. Evaluation of carum-loaded niosomes on breast cancer cells: Physicochemical properties, in vitro cytotoxicity, flow cytometric, DNA fragmentation and cell migration assay. Scientific reports. 2019;9(1):1-10.
[11] Mashayekhi S, Rasoulpoor S, Shabani S, Esmaeilizadeh N, Serati-Nouri H, Sheervalilou R, *et al.* Curcumin-loaded mesoporous silica nanoparticles/nanofiber composites for supporting long-term proliferation and stemness preservation of adipose-derived stem cells. Int J Pharm. 2020;587:119656.
[12] Shakeri-Zadeh A, Zareyi H, Sheervalilou R, Laurent S, Ghaznavi H, Samadian H. Gold nanoparticle-mediated bubbles in cancer nanotechnology. Journal of Controlled Release. 2020.
[13] Irajirad R, Ahmadi A, Najafabad BK, Abed Z, Sheervalilou R, Khoei S, *et al.* Combined thermo-chemotherapy of cancer using 1 MHz ultrasound waves and a cisplatin-loaded sonosensitizing nanoplatform: an in vivo study. Cancer chemotherapy and pharmacology. 2019;84(6):1315-21.
[14] Shirvalilou S, Khoei S, Esfahani AJ, Kamali M, Shirvaliloo M, Sheervalilou R, *et al.* Magnetic Hyperthermia as an adjuvant cancer therapy in combination with radiotherapy versus radiotherapy alone for recurrent/progressive glioblastoma: a systematic review. J Neuro-Oncology. 2021:1-10.
[15] Dasari S, Tchounwou PBJEjop. Cisplatin in cancer therapy: molecular mechanisms of action. 2014;740:364-78.
[16] Dhar S, Kolishetti N, Lippard SJ, Farokhzad OCJPotNAoS. Targeted delivery of a cisplatin prodrug for safer and more effective prostate cancer therapy in vivo. 2011;108(5):1850-5.
[17] Barani M, Mirzaei M, Torkzadeh-Mahani M, Lohrasbi-Nejad A, Nematollahi MH. A new formulation of hydrophobin-coated niosome as a drug carrier to cancer cells. Materials Sci Eng: C. 2020;113:110975.
[18] Barani M, Mukhtar M, Rahdar A, Sargazi G, Thysiadou A, Kyzas GZ. Progress in the Application of Nanoparticles and Graphene as Drug Carriers and on the Diagnosis of Brain Infections. Molecules. 2021;26(1):186.
[19] Barani M, Nematollahi MH, Zaboli M, Mirzaei M, Torkzadeh-Mahani M, Pardakhty A, *et al.* In silico and in vitro study of magnetic niosomes for gene delivery: The effect of ergosterol and cholesterol. Mat Sci Eng: C. 2019;94:234-46.
[20] Barani M, Sabir F, Rahdar A, Arshad R, Kyzas GZ. Nanotreatment and nanodiagnosis of prostate cancer: recent updates. Nanomaterials. 2020;10(9):1696.
[21] Chauhan NPS, Jadoun S, Rathore BS, Barani M, Zarrintaj P. Redox polymers for capacitive energy storage applications. J Energy Storage. 2021;43:103218.
[22] Das SS, Bharadwaj P, Bilal M, Barani M, Rahdar A, Taboada P, et al. Stimuli-responsive polymeric nanocarriers for drug delivery, imaging, and theragnosis. Polymers. 2020;12(6):1397.
[23] Davarpanah F, Yazdi AK, Barani M, Mirzaei M, Torkzadeh-Mahani M. Magnetic delivery of antitumor carboplatin by using PEGylated-Niosomes. DARU J Pharm Sci. 2018;26(1):57-64.
[24] Ebrahimi AK, Barani M, Sheikhshoaie I. Fabrication of a new superparamagnetic metal-organic framework with core-shell nanocomposite structures: Characterization, biocompatibility, and drug release study. Mat Sci Eng: C. 2018;92:349-55.
[25] Hajizadeh MR, Maleki H, Barani M, Fahmidehkar MA, Mahmoodi M, Torkzadeh-Mahani M. In vitro cytotoxicity assay of D-limonene niosomes: an efficient nano-carrier for enhancing solubility of plant-extracted agents. Research in Pharm Sci. 2019;14(5):448.
[26] Hajizadeh MR, Parvaz N, Barani M, Khoshdel A, Fahmidehkar MA, Mahmoodi M, *et al.* Diosgenin-loaded niosome as an effective phytochemical nanocarrier: Physicochemical characterization, loading efficiency, and cytotoxicity assay. DARU J Pharm Sci. 2019;27(1):329-39.
[27] Chiani M, Milani AT, Nemati M, Rezaeidian J, Ehsanbakhsh H, Ahmadi Z, *et al.* Anticancer effect of cisplatin-loaded poly (Butyl-cyanoacrylate) nanoparticles on A172 brain cancer cells line. 2019;20(1):303.
[28] Rahdar A, Hajinezhad MR, Sivasankarapillai VS, Askari F, Noura M, Kyzas GZ. Synthesis, characterization, and intraperitoneal biochemical studies of zinc oxide nanoparticles in Rattus norvegicus. Applied Physics A. 2020;126(5):1-9.
[29] Salimi A, Zadeh BSM, Godazgari S, Rahdar A. Development and Evaluation of Azelaic Acid-Loaded Microemulsion for Transfollicular Drug Delivery Through Guinea Pig Skin: A Mechanistic Study. Adv Pharm bulletin. 2020;10(2):239.
[30] Sivasankarapillai V, Das S, Sabir F, Sundaramahalingam M, Colmenares J, Prasannakumar S, *et al.* Progress in natural polymer engineered biomaterials for transdermal drug delivery systems. Materials Today Chemistry. 2021;19:100382.
[31] Sivasankarapillai VS, Pillai AM, Rahdar A, Sobha AP, Das SS, Mitropoulos AC, *et al.* On facing the SARS-CoV-2 (COVID-19) with combination of nanomaterials and medicine: possible strategies and first challenges. Nanomaterials. 2020;10(5):852.
[32] Taimoory SM, Rahdar A, Aliahmad M, Sadeghfar F, Hajinezhad MR, Jahantigh M, *et al.* The synthesis and characterization of a magnetite nanoparticle with potent antibacterial activity and low mammalian toxicity. J Molecular Liquids. 2018;265:96-104.
[33] Farooq MA, Aquib M, Farooq A, Haleem Khan D, Joelle Maviah MB, Sied Filli M, *et al.* Recent progress in nanotechnology-based novel drug delivery systems in designing of cisplatin for cancer therapy: an overview. 2019;47(1):1674-92.
[34] Hasanein P, Rahdar A, Barani M, Baino F, Yari S. Oil-in-water microemulsion encapsulation of antagonist drugs prevents renal ischemia-reperfusion injury in rats. Appl Sci. 2021;11(3):1264.
[35] Hosseinikhah SM, Barani M, Rahdar A, Madry H, Arshad R, Mohammadzadeh V, *et al.* Nanomaterials for the Diagnosis and Treatment of Inflammatory Arthritis. Int J Molecular Sci. 2021;22(6):3092.

[36] Motamedi N, Barani M, Lohrasbi-Nejad A, Mortazavi M, Riahi-Medvar A, Varma RS, *et al.* Enhancement of thermostability of aspergillus flavus urate oxidase by immobilization on the Ni-based magnetic metal–organic framework. Nanomaterials. 2021;11(7):1759.
[37] Mukhtar M, Bilal M, Rahdar A, Barani M, Arshad R, Behl T, et al. Nanomaterials for diagnosis and treatment of brain cancer: Recent updates. Chemosensors. 2020;8(4):117.
[38] Nikazar S, Barani M, Rahdar A, Zoghi M, Kyzas GZ. Photo-and Magnetothermally Responsive Nanomaterials for Therapy, Controlled Drug Delivery and Imaging Applications. ChemistrySelect. 2020;5(40):12590-609.
[39] Okey-Onyesolu CF, Hassanisaadi M, Bilal M, Barani M, Rahdar A, Iqbal J, *et al.* Nanomaterials as Nanofertilizers and Nanopesticides: An Overview. ChemistrySelect. 2021;6(33):8645-63.
[40] Qindeel M, Barani M, Rahdar A, Arshad R, Cucchiarini M. Nanomaterials for the diagnosis and treatment of urinary tract infections. Nanomaterials. 2021;11(2):546.
[41] Rahdar A, Hajinezhad MR, Nasri S, Beyzaei H, Barani M, Trant JF. The synthesis of methotrexate-loaded F127 microemulsions and their in vivo toxicity in a rat model. J Molecular Liquids. 2020;313:113449.
[42] Rahdar A, Taboada P, Hajinezhad MR, Barani M, Beyzaei H. Effect of tocopherol on the properties of Pluronic F127 microemulsions: Physico-chemical characterization and in vivo toxicity. J Molecular Liquids. 2019;277:624-30.
[43] Sabir F, Barani M, Mukhtar M, Rahdar A, Cucchiarini M, Zafar MN, *et al.* Nanodiagnosis and nanotreatment of cardiovascular diseases: An overview. Chemosensors. 2021;9(4):67.
[44] Babaei M, Akbarzade A, Arjmand M, Safekordi A. Effect Of Cisplatin Niosome And Cisplatin Niosome Polyethylenglycol On A172 Cell Line. 2014.
[45] Ag Seleci D, Seleci M, Walter J-G, Stahl F, Scheper TJJon. Niosomes as nanoparticular drug carriers: fundamentals and recent applications. 2016.
[46] Sabir F, Qindeel M, Zeeshan M, Ul Ain Q, Rahdar A, Barani M, et al. Onco-Receptors Targeting in Lung Cancer via Application of Surface-Modified and Hybrid Nanoparticles: A Cross-Disciplinary Review. Processes. 2021;9(4):621.
[47] Sabir F, Zeeshan M, Laraib U, Barani M, Rahdar A, Cucchiarini M, *et al.* DNA based and stimuli-responsive smart nanocarrier for diagnosis and treatment of cancer: Applications and challenges. Cancers. 2021;13(14):3396.
[48] Sharma V, Dash SK, Govarthanan K, Gahtori R, Negi N, Barani M, *et al.* Recent Advances in Cardiac Tissue Engineering for the Management of Myocardium Infarction. Cells. 2021;10(10):2538.
[49] Torkzadeh-Mahani M, Zaboli M, Barani M, Torkzadeh-Mahani M. A combined theoretical and experimental study to improve the thermal stability of recombinant D-lactate dehydrogenase immobilized on a novel superparamagnetic Fe3O4NPs@ metal–organic framework. Applied Organometallic Chemistry. 2020;34(5):e5581.
[50] Zeraati M, Kazemzadeh P, Barani M, Sargazi G. Selecting the appropriate carbon source in the synthesis of SiC nano-powders using an optimized Fuzzy Model. Silicon. 2021:1-12.
[51] Akbari A, Sabouri Z, Hosseini HA, Hashemzadeh A, Khatami M, Darroudi M. Effect of nickel oxide nanoparticles as a photocatalyst in dyes degradation and evaluation of effective parameters in their removal from aqueous environments. Inorganic Chemistry Communications. 2020;115:107867.
[52] Alijani HQ, Pourseyedi S, Mahani MT, Khatami M. Green synthesis of zinc sulfide (ZnS) nanoparticles using Stevia rebaudiana Bertoni and evaluation of its cytotoxic properties. J Molecular Structure. 2019;1175:214-8.
[53] Alijani HQ, Pourseyedi S, Torkzadeh-Mahani M, Seifalian A, Khatami M. Bimetallic nickel-ferrite nanorod particles: greener synthesis using rosemary and its biomedical efficiency. Artificial cells, nanomedicine, and biotechnology. 2020;48(1):242-51.
[54] Alkasir M, Samadi N, Sabouri Z, Mardani Z, Khatami M, Darroudi M. Evaluation cytotoxicity effects of biosynthesized zinc oxide nanoparticles using aqueous Linum Usitatissimum extract and investigation of their photocatalytic activityackn. Inorganic Chemistry Communications. 2020;119:108066.
[55] Das SS, Bharadwaj P, Bilal M, Barani M, Rahdar A, Taboada P, et al. Stimuli-responsive polymeric nanocarriers for drug delivery, imaging, and theragnosis. 2020;12(6):1397.
[56] Cosco D, Paolino D, Muzzalupo R, Celia C, Citraro R, Caponio D, *et al.* Novel PEG-coated niosomes based on bola-surfactant as drug carriers for 5-fluorouracil. 2009;11(5):1115-25.
[57] Gude R, Jadhav M, Rao S, Jagtap AJCB, Radiopharmaceuticals. Effects of niosomal cisplatin and combination of the same with theophylline and with activated macrophages in murine B16F10 melanoma model. 2002;17(2):183-92.
[58] Yang H, Deng A, Zhang J, Wang J, Lu BJJom. Preparation, characterization and anticancer therapeutic efficacy of cisplatin-loaded niosomes. 2013;30(3):237-44.
[59] Catanzaro D, Nicolosi S, Cocetta V, Salvalaio M, Pagetta A, Ragazzi E, *et al.* Cisplatin liposome and 6-amino nicotinamide combination to overcome drug resistance in ovarian cancer cells. Oncotarget. 2018;9(24):16847.
[60] Huo T, Barth RF, Yang W, Nakkula RJ, Koynova R, Tenchov B, et al. Preparation, biodistribution and neurotoxicity of liposomal cisplatin following convection enhanced delivery in normal and F98 glioma bearing rats. PloS one. 2012;7(11):e48752.
[61] Haghighat M, Alijani HQ, Ghasemi M, Khosravi S, Borhani F, Sharifi F, *et al.* Cytotoxicity properties of plant-mediated synthesized K-doped ZnO nanostructures. Bioprocess and Biosystems Engineering. 2021:1-9.
[62] Alahri MB, Arshadizadeh R, Raeisi M, Khatami M, Sajadi MS, Abdelbasset WK, *et al.* Theranostic applications of metal-organic frameworks (MOFs)-based materials in brain disorders: recent advances and challenges. Inorganic Chemistry Communications. 2021:108997.
[63] Sabouri Z, Rangrazi A, Amiri MS, Khatami M, Darroudi M. Green synthesis of nickel oxide nanoparticles using Salvia hispanica L.(chia) seeds extract and studies of their photocatalytic activity and cytotoxicity effects. Bioprocess and Biosystems Engineering. 2021;44(11):2407-15.
[64] Sargazi S, Hajinezhad MR, Barani M, Rahdar A, Shahraki S, Karimi P, *et al.* Synthesis, characterization, toxicity and morphology assessments of newly prepared microemulsion systems for delivery of valproic acid. Journal of Molecular Liquids. 2021;338:116625.
[65] Barani M, Sangiovanni E, Angarano M, Rajizadeh MA, Mehrabani M, Piazza S, *et al.* Phytosomes as Innovative Delivery Systems for Phytochemicals: A Comprehensive Review of Literature. International Journal of Nanomedicine. 2021;16:6983-7022.
[66] Zarrintaj P, Ghorbani S, Barani M, Singh Chauhan NP, Khodadadi Yazdi M, Saeb MR, *et al.* Polylysine for Skin Regeneration: A Review of Recent Advances and Perspectives. Bioengineering &

Translational Medicine.e10261.
[67] Ouyang D, Smith SC. Introduction to computational pharmaceutics. Computational Pharmaceutics. 2015:1-5.
[68] Villalobos R, V Garcia E, Quintanar D, M Young P. Drug release from inert spherical matrix systems using Monte Carlo simulations. Current drug delivery. 2017;14(1):65-72.
[69] Dickson CJ, Madej BD, Skjevik ÅA, Betz RM, Teigen K, Gould IR, *et al.* Lipid14: the amber lipid force field. Journal of chemical theory and computation. 2014;10(2):865-79.
[70] Vanquelef E, Simon S, Marquant G, Garcia E, Klimerak G, Delepine JC, *et al.* RED Server: a web service for deriving RESP and ESP charges and building force field libraries for new molecules and molecular fragments. Nucleic Acids Res. 2011;39(suppl_2):W511-W7.
[71] Sousa da Silva AW, Vranken WF. ACPYPE - AnteChamber PYthon Parser interfacE. BMC Research Notes. 2012;5(1):367.
[72] Li P, Merz KM, Jr. MCPB.py: A Python Based Metal Center Parameter Builder. J Chem Inf Model. 2016;56(4):599-604.
[73] Case D, Pearlman D, Caldwell J. Amber 18.(2018) University of California. San Francisco.
[74] Sommer Br, Dingersen T, Gamroth C, Schneider SE, Rubert S, Kruğer J, *et al.* CELLmicrocosmos 2.2 MembraneEditor: a modular interactive shape-based software approach to solve heterogeneous membrane packing problems. Journal of chemical information and modeling. 2011;51(5):1165-82.
[75] Chen F, Smith PE. Simulated surface tensions of common water models. American Institute of Physics; 2007.
[76] Nasseri B. Effect of cholesterol and temperature on the elastic properties of niosomal membranes. International journal of pharmaceutics. 2005;300(1-2):95-101.
[77] Baranyai A, Evans DJ. New algorithm for constrained molecular-dynamics simulation of liquid benzene and naphthalene. Molecular Physics. 1990;70(1):53-63.
[78] Berendsen HJ, van der Spoel D, van Drunen R. GROMACS: a message-passing parallel molecular dynamics implementation. Computer physics communications. 1995;91(1-3):43-56.
[79] Mosmann T. Rapid colorimetric assay for cellular growth and survival: application to proliferation and cytotoxicity assays. Journal of immunological methods. 1983;65(1-2):55-63.
[80] Peltonen L, Hirvonen J, Yliruusi J. The effect of temperature on sorbitan surfactant monolayers. Journal of colloid and interface science. 2001;239(1):134-8.
[81] Allen WJ, Lemkul JA, Bevan DR. GridMAT-MD: a grid-based membrane analysis tool for use with molecular dynamics. Journal of computational chemistry. 2009;30(12):1952-8.
[82] Aferni AE, Guettari M, Tajouri T, Rahdar A. The confinement of PVP in AOT microemulsions: Effect of water content and PVP concentration regime on electrical percolation phenomenon. J Molecular Liquids. 2020;318:114012.
[83] Arshad R, Pal K, Sabir F, Rahdar A, Bilal M, Shahnaz G, *et al.* A review of the nanomaterials use for the diagnosis and therapy of salmonella typhi. J Molecular Structure. 2021:129928.
[84] Heydari M, Yousefi AR, Rahdar A, Nikfarjam N, Jamshidi K, Bilal M, *et al.* Microemulsions of tribenuron-methyl using Pluronic F127: Physico-chemical characterization and efficiency on wheat weed. J Molecular Liquids. 2021;326:115263.
[85] Pillai AM, Sivasankarapillai VS, Rahdar A, Joseph J, Sadeghfar F, Rajesh K, *et al.* Green synthesis and characterization of zinc oxide nanoparticles with antibacterial and antifungal activity. J Molecular Structure. 2020;1211:128107.
[86] Rahdar A, Aliahmad M, Samani M, HeidariMajd M, Susan MABH. Synthesis and characterization of highly efficacious Fe-doped ceria nanoparticles for cytotoxic and antifungal activity. Ceramics International. 2019;45(6):7950-5.
[87] Rahdar A, Beyzaei H, Askari F, Kyzas GZ. Gum-based cerium oxide nanoparticles for antimicrobial assay. Applied Physics A. 2020;126(5):1-9.
[88] Moghaddam FD, Akbarzadeh I, Marzbankia E, Farid M, Reihani AH, Javidfar M, *et al.* Delivery of melittin-loaded niosomes for breast cancer treatment: an in vitro and in vivo evaluation of anti-cancer effect. 2021;12(1):1-35.
[89] Mandriota G, Di Corato R, Benedetti M, De Castro F, Fanizzi FP, Rinaldi RJAam, *et al.* Design and application of cisplatin-loaded magnetic nanoparticle clusters for smart chemotherapy. 2018;11(2):1864-75.
[90] Doijad R, Manvi F, Swati S, Rony MJId. Niosomal drug delivery of Cisplatin: Development and characterization. 2008;45(9):713-8.
[91] Al-Bahlani SM, Al-Bulushi KH, Al-Alawi ZM, Al-Abri NY, Al-Hadidi ZR, Al-Rawahi SS. Cisplatin induces apoptosis through the endoplasmic reticulum-mediated, calpain 1 pathway in triple-negative breast cancer cells. Clinical Breast Cancer. 2017;17(3):e103-e12.
[92] Ag Seleci D, Seleci M, Walter J-G, Stahl F, Scheper T. Niosomes as nanoparticular drug carriers: fundamentals and recent applications. J nanomaterials. 2016;2016.
[93] Kanaani L, Tabrizi MM, Khiyavi AA, Javadi I. Improving the Efficacy of Cisplatin using Niosome Nanoparticles Against Human Breast Cancer Cell Line BT-20: An In Vitro Study. Asian Pacific J Cancer Biology. 2017;2(2):27-9.
[94] Yang H, Deng A, Zhang J, Wang J, Lu B. Preparation, characterization and anticancer therapeutic efficacy of cisplatin-loaded niosomes. J microencapsulation. 2013;30(3):237-44.
[95] Ciarimboli G. Membrane transporters as mediators of cisplatin side-effects. Anticancer research. 2014;34(1):547-50.
[96] Gude R, Jadhav M, Rao S, Jagtap A. Effects of niosomal cisplatin and combination of the same with theophylline and with activated macrophages in murine B16F10 melanoma model. Cancer Biotherapy and Radiopharmaceuticals. 2002;17(2):183-92.
[97] Marianecci C, Di Marzio L, Rinaldi F, Celia C, Paolino D, Alhaique F, *et al.* Niosomes from 80s to present: the state of the art. Advances in colloid and interface science. 2014;205:187-206.
[98] Khoee S, Yaghoobian M. Niosomes: A novel approach in modern drug delivery systems. Nanostructures for drug delivery: Elsevier; 2017. p. 207-37.